Characterisation of Cardiac Health in the Reduced Uterine Perfusion Pressure Model and a 3D Cardiac Spheroid Model, of Preeclampsia

Claire Richards
University of Technology Sydney Faculty of Science https://orcid.org/0000-0001-5080-9164
Kimberly Sesperez
University of Technology Sydney Faculty of Science
Michael Chhor
University of Technology Sydney Faculty of Science
Sahar Ghorbanpour
University of Technology Sydney Faculty of Science
Claire Rennie
University of Technology Sydney Faculty of Science
Clara Liu Chung Ming
University of Technology Sydney Faculty of Engineering: University of Technology Sydney Faculty of Engineering and Information Technology
Chris Evenhuis
University of Technology Sydney
Valentina N Nikolic
University of Nis: Univerzitet u Nisu
Natasa Karadzov Orlic
University of Belgrade: Univerzitet u Beogradu
Zeljko Mikovic
University of Belgrade: Univerzitet u Beogradu
Milan Stefanovic
University of Nis: Univerzitet u Nisu
Zoran Cakic
University of Niš: Univerzitet u Nisu
Kristine McGrath
University of Technology Sydney Faculty of Science
Carmine Gentile
University of Technology Sydney Faculty of Engineering: University of Technology Sydney Faculty of Engineering and Information Technology
Kristen Bubb
Monash University
Lana McClements (lana.mcclements@uts.edu.au)
University of Technology Sydney Faculty of Science https://orcid.org/0000-0002-4911-1014

Research

Keywords: Preeclampsia, cardiovascular disease, reduced uterine perfusion pressure, cardiac spheroids, FKBPL

Posted Date: December 30th, 2020

DOI: https://doi.org/10.21203/rs.3.rs-135799/v1

Version of Record: A version of this preprint was published at Biology of Sex Differences on April 20th, 2021. See the published version at https://doi.org/10.1186/s13293-021-00376-1.

Abstract

Background: Preeclampsia is a life-threatening cardiovascular disorder of pregnancy that leads to an increased risk of ongoing cardiovascular and metabolic disorders. Much of the pathogenesis and mechanisms involved in cardiac health are unknown. A novel anti-angiogenic protein, FKBPL, is emerging as having a potential role in both preeclampsia and cardiovascular disease (CVD). Therefore, in this study we aimed to investigate the role of FKBPL in cardiac health in the rat reduced uterine perfusion pressure (RUPP) model and 3D cardiac spheroid model, of preeclampsia.

Methods: The RUPP model was induced in pregnant rats and histological analysis performed on the heart, kidneys, liver and placenta ($n \geq 6$). Picrosirius red staining was performed to quantify collagen I/III deposition in rat hearts, placentae and livers as an indicator of fibrosis. RT-qPCR was used to determine changes in *Fkbpl*, *Icam1*, *Vcam1, Flt1* and/or *Vegfa* mRNA in hearts and/or placentae and ELISA was used to evaluate cardiac brain natriuretic peptide (BNP45) and FKBPL secretion in rat hearts. Cardiac spheroids were generated using human cardiac fibroblasts (HCFs) and human coronary artery endothelial cells (HCAECs) and treated with patient plasma from normotensive controls, early-onset preeclampsia (EOPE) and late-onset preeclampsia (LOPE); (n=3). FKBPL and CD31 expression was quantified by immunofluorescent labelling.

Results: The RUPP procedure induced significant increase in blood pressure ($p<0.001$), cardiac collagen deposition ($p<0.001$) and cardiac BNP45 ($p<0.05$). It also induced a significant increase in cardiac FKBPL mRNA expression ($p<0.05$) and protein levels ($p<0.01$). RUPP placentae also exhibited increased collagen deposition and decreased *Flt1* mRNA expression ($p<0.05$). RUPP kidneys revealed an increase in average glomerular size ($p<0.05$). Cardiac spheroids showed a significant increase in FKBPL expression when treated with LOPE patient plasma ($p<0.05$) and a trend towards increased FKBPL expression following treatment with EOPE plasma ($p=0.06$).

Conclusions: The rat RUPP model induced cardiac, renal and placental features reflective of preeclampsia in humans. FKBPL was increased in the hearts of RUPP rats and in cardiac spheroids treated with plasma from women with preeclampsia, reflective of restricted angiogenesis in this disorder. Elucidation of this novel FKBPL mechanism in cardiac health in preeclampsia could be key in preventing future CVD.

Background

Preeclampsia is a dangerous cardiovascular disorder of pregnancy that affects around 5–8% of pregnancies and is one of the leading causes of maternal and foetal morbidity and mortality worldwide[1]. Preeclampsia typically presents during the second half of pregnancy (> 20 weeks) and is characterised by the new-onset of hypertension (> 140/90 mmHg) in the presence of proteinuria (> 300 mg/day) or other end-organ dysfunction, often that of the liver and kidneys[2, 3]. While low-dose aspirin has been investigated as a potential preventative treatment, the only cure for preeclampsia remains the delivery of the placenta and the baby, which is often at pre-term[4–6]. In addition to the immediate complications of a pregnancy affected by preeclampsia, women and babies affected by this disease are at a greater risk of developing post-partum cardiovascular, metabolic and neurological disorders[7–11]. In fact, women who are diagnosed with early-onset preeclampsia (EOPE; presenting prior to 34 weeks gestation) are at 9–10 fold increased risk of cardiovascular disease (CVD)-related deaths, while women diagnosed with late-onset preeclampsia (LOPE; presenting after 34 weeks gestation) are at a 2-fold increased risk of CVD-related death compared to those with normotensive pregnancies[12, 13]. Recently, several overlapping pathways and systems were identified between preeclampsia, hypertension and heart failure with preserved ejection fraction (HFpEF)[14, 15].

Preeclampsia generally presents with two phenotypes: EOPE and LOPE; although term preeclampsia can also occur. While the delineation of these two phenotypes is still under investigation, EOPE often presents with a more severe disease state due to poor placentation and intrauterine growth restriction (IUGR) while LOPE results from poor maternal vascular

adaptation and a predisposition to CVD[16]. Even though the complex pathogenesis of this disease remains unknown, inappropriate placental development due to poor invasion and remodelling of maternal uterine vasculature and inability of the mother's cardiovascular system to adapt to pregnancy-induced changes, appear to have critical roles. These factors result in aberrant angiogenesis, oxidative stress and inflammatory responses[17]. Anti-angiogenic factors including soluble fms-like tyrosine kinase-1 (sFlt-1) and soluble endoglin (sEng) are upregulated in preeclampsia and induce their effects by blocking the angiogenesis-promoting actions of vascular endothelial growth factor (VEGF) and placental growth factor (PlGF)[18].

A novel anti-angiogenic protein, FK506-binding protein like (FKBPL), has recently been identified as having predictive and diagnostic roles in preeclampsia[19] as well as being a determinant of CVD[20]. FKBPL is a divergent member of the immunophilin group that shares similar structure and functions to the FKBP members but lacks an essential residue in its PPI domain preventing its ability to exert this catalytic activity[21]. FKBPL has been demonstrated to have many functions including regulating glucocorticoid, androgen and oestrogen receptors as well as angiogenesis and stem cell differentiation[22–26]. It has been demonstrated that FKBPL induces anti-angiogenic effects by binding to the cluster of differentiation 44 (CD44) receptor on the surface of cells[27, 28]. While we have shown FKBPL to be more highly expressed in women with preeclampsia, its specific function in cardiovascular health in preeclampsia is unknown[19].

In this study, we demonstrate in the RUPP model of preeclampsia, the presence of diastolic dysfunction and cardiac fibrosis in association with increased cardiac FKBPL expression and secretion. We further show that cardiac spheroids containing cardiac fibroblasts and endothelial cells, treated with plasma samples from women with EOPE or LOPE, express higher levels of FKBPL protein reflective of restricted angiogenesis.

Methods

Experimental animals

All animal experiments were approved by the Northern Sydney Local Health District Animal Ethics Committee (Animal Ethics number: RESP/18/317). Time-mated pregnant rats were acquired from the Animal Resources Centre (ARC) and arrived between days 7–10 of pregnancy. They were housed within the Kearns Facility at the Kolling Institute of Medical Research and were fed a standard sterile chow diet and accessed water *ad libitum*. Pregnant rats were randomised to the Sham or RUPP procedure. At gestational day (GD) 14, the RUPP operation was performed as previously described [29, 30]. Briefly, silver clips were applied to the aorta above the iliac bifurcation (0.203 mm ID) and both the right and left uterine arcades (0.100 mm ID) to reduce the blood flow to the uterus by ~ 40%. The sham procedure was performed by making a midline incision to open the lower abdominal cavity, though no clips were applied. On GD19, pregnant rats were anaesthetised with isoflurane (2–5% inhalation), and placed on a warm pad to maintain body temperature of 37ºC before echocardiography was performed. They were allowed to recover from the brief anaesthetic for several hours before being anaesthetised again later in the day for the implantation of a chronic indwelling catheter, inserted into the carotid artery for blood pressure measurement. After clinical phenotyping was completed, rats were euthanized and blood, urine, organs, placentae and embryos collected and stored in paraformaldehyde and liquid nitrogen. Hearts, placentae and embryos were also weighed before being processed.

Echocardiography

Cardiac morphology and function were measured by paraventricular short and long axis echocardiography in M-mode and B-mode, respectively, using a VisualSonics Vevo 3100 echocardiography system. Stroke volume (µl), cardiac output (mL/min), LV ejection fraction (%), fractional shortening (%), LV mass (mg) and LV anterior and posterior wall thicknesses at diastole (d) and systole (s) were measured from short-axis M-mode images.

Histology

Organs were formalin fixed, processed using Excelsior AS Tissue Processor (Thermo Fisher Scientific, USA), embedded in paraffin wax and stored at room temperature. Tissue sections (10 µm) were subjected to haematoxylin and eosin staining to visualise tissue morphology. Images were taken using a ZEISS Axioscan microscope. The size of 50 glomeruli per sample were measured using the polygon tool in Zen Lite 3.2 software to generate 2-dimensional surface area measurements. Overall cell number and cell size were measured in rat H&E stained liver sections using ImageJ. Picrosirius red staining was also performed to identify collagen I/III fibres as markers of fibrosis. Quantification of collagen fibres was performed using the colour threshold function of ImageJ.

Brain natriuretic peptide (BNP) 45 Enzyme-linked immunosorbent assay (ELISA)

Rat cardiac lysates were used to measure BNP 45 concentrations in rat hearts using BNP 45 Rat ELISA Kit (Abcam, product #ab108816, United Kingdom) as per the manufacturer's instructions. Briefly, all reagents, standards, and samples were prepared as per the assay protocols. Standard and heart protein samples were added to each well, incubated and washed with washing buffer. Biotinylated BNP 45 antibody was added to each well, incubated and washed. Next, streptavidin-peroxidase conjugate was added to each well, incubated and washed. Finally, chromogen substrate was added and briefly incubated until colour change occurred. Stopping solution was added to stop the reaction and immediately after, optical density was detected using the Tecan infinite M200PRO, (Tecan Austria, GmbH) microplate reader.

FKBPL ELISA

Specific FKBPL protein concentrations of rat hearts were measured by indirect ELISA developed in-house using a DuoSet® Ancillary Reagent Kit 1 (R&D Systems, USA). Briefly, PBS-diluted standards and samples were added to each well of a 96 well plate (Immulon 1B, Flat bottom Microtiter plates, 3355). The plate was incubated overnight on a shaker at 4 °C. The following day, the plate was washed with 1X wash buffer before blocking buffer was added and incubated on a shaker for 2hr at room temperature. The plate was then washed with 1X wash buffer before primary antibody (Rabbit FKBPL Polyclonal antibody, Cat No. 10060-1-AP, 0.4 µg/ml in 1% BSA) was added to each well and incubated on a shaker for 2 hr at room temperature. The plate was washed before the secondary antibody was applied (Anti-Rabbit: ab205722, 2 mg/ml, Dnk PAb to Rb IgG (HRP)), 100 ng/ml in 1% BSA) followed by shaking for 2hr at room temperature. The plate was washed, and Colour Reagent A and Colour Reagent B were mixed in 1:1 and added to each well before incubating in the dark for 20 min at room temperature. Following incubation, stop solution was added and the absorbance measured at 450 nm and 540 nm using a Tecan infinite M200PRO, (Tecan Austria, GmbH) microplate reader. The concentration of unknown samples was calculated based on a Sigmoidal standard curve generated from the protein standards.

Quantitative reverse transcription polymerase chain reaction (RT-qPCR)

RT-qPCR was used to analyse mRNA expression of the genes *Fkbpl*, *intercellular adhesion molecule 1* (*Icam1)*, *vascular cell adhesion protein 1* (*Vcam1)*, fms-like tyrosine kinase 1 (*Flt1*, aka vascular endothelial growth factor receptor 1; Vegfr1) and *vascular endothelial growth factor a (Vegfa)* in the heart and/or placental tissue of the Sham and RUPP rats. RNA was extracted from the tissue by homogenising tissue sections with TRIsure reagent (Bioline, AU) and purified according to the manufacturer's protocol. Extracted RNA was converted to cDNA by reverse transcription using Tetro cDNA synthesis kit (Bioline, AU) and corresponding primers for: *Fkbpl* (sense, 5'- TGGCCTCTCAGGTCTGAACTA-3'; antisense, 5'-TGGGGACTGCTGCTTAATCG-3'), *Icam1* (sense, 5'-ATGTGCTATATGGTCCTCAC-3'; antisense, 5'-GTTTGACAGACTTCACCATC-3'), *Vcam1* (sense, 5'-CTGATTATCCAAGGCTCTTC-3'; antisense, 5'-CCATTAACAGACTTTAGCACC-3'), *Flt1* (sense, 5'-CCAGAAGTCGTATGGTTAAAAG-3'; antisense, 5'-GCTGTGAGGTTTCTAAATAGC-3') and *Vegfa* (sense, 5'-GATAGAGTATATCTTCAAGCCG-3'; antisense, 5'-

CTCATCTCTCCTATGTGCTG-3'). Real-time polymerase chain reaction (RT-PCR) was conducted using the prepared cDNA using a SensiFAST SYBR No-ROX Kit (Bioline, AU) according to the manufacturer's protocol.

Generation and staining of cardiac spheroids

Cardiac spheroids were generated by co-culturing human cardiac fibroblasts (HCFs) with human coronary artery endothelial cells (HCAECs) in hanging drop cultures at a ratio of 1:1 similar to the human heart. Hanging drop cultures were generated using Perfecta 3D® 96 well hanging drop plates (3D Biomatrix, Ann Arbor, MI, USA). The spheroids were maintained with fresh growth medium every two days and placed in a 37 °C incubator. Treatment of patient plasma serum was performed after spheroids were formed (3 days) as previously described[31]. Spheroids remained in incubation with plasma for 6 days. Cardiac spheroids were fixed using 1X PBS containing 4% paraformaldehyde, washed in PBS/0.01% sodium azide (PBSA), permeabilised using PBSA containing 0.02% Triton X-100, and blocked with 3% BSA in PBSA. Spheroids were incubated with appropriate primary (Anti-FKBPL rabbit pAb, Proteintech UK; Anti-CD31 mouse mAb, BD Biosciences, USA) and secondary (Anti-rabbit Donkey Cy3 conjugated, Abcam, UK; Anti-mouse Donkey Alexa-fluor conjugated, Thermo Fisher, USA) antibodies, and nuclei stained using Hoechst stain.

Human plasma samples

Plasma samples from women with EOPE (before 34 weeks' gestation) or LOPE (after 34 weeks' gestation) were collected following the diagnosis. Preeclampsia was defined according to the 2013 ACOG guidelines by the clinicians in participating hospitals[32]. The study was approved by the local institutional review boards and written informed consent was obtained from all participants as per the principles outlined in the Declaration of Helsinki.

Statistical analysis

Statistical analysis was performed in GraphPad Prism (v5). For analyses requiring comparison of the Sham and RUPP groups, an unpaired student's t-test was performed with statistically significant results equivalent to a p-value of 0.05 or less. Where $n \leq 4$, a Mann-Whitney t-test was performed.

Results

RUPP procedure induces altered cardiovascular physiology in rats

To assess whether the RUPP procedure was successful in inducing preeclampsia and associated cardiovascular changes in rats, blood pressure was measured on GD19 in both RUPP ($n = 6$) and sham surgery (n = 8) rats. Table 1 demonstrates that systolic blood pressure, diastolic blood pressure, mean arterial blood pressure (MABP) and heart rate were all significantly increased in RUPP rats compared to sham control rats.

Table 1
Maternal cardiac data in reduced uterine perfusion pressure rat model

	Sham ($n = 7$)	RUPP ($n \geq 4$)	P Value
Maternal body weight, g	338.6 ± 17.5	379.5 ± 4.87	0.0843
Maternal heart weight, g	1.02 ± 0.05	1.224 ± 0.01	**0.0081****
Heart: Body weight, %	0.304 ± 0.01	0.323 ± 0.005	0.3032
Heart rate, bpm	369.3 ± 4.8	398.8 ± 3.7	**0.0006*****
Systolic BP, mmHg	112.6 ± 1.3	127.8 ± 1.9	**< 0.0001*****
Diastolic BP, mmHg	87.6 ± 1.7	104.0 ± 1.8	**< 0.0001*****
MABP, mmHg	100.9 ± 1.5	116.7 ± 1.7	**< 0.0001*****
Stroke volume, µl	215.0 ± 4.326	230.0 ± 13.26	0.304
Cardiac output, mL/min	79 ± 3	85 ± 5	0.0669
Ejection fraction, %	82 ± 2	78 ± 2	0.2333
Fractional shortening, %	52 ± 2	49 ± 2	0.2363
Corrected LV mass, mg	600 ± 14	706 ± 68	**0.0373***
LV anterior wall systolic, mm	2.9 ± 0.12	2.9 ± 0.11	0.6725
LV anterior wall diastolic, mm	1.5 ± 0.04	1.8 ± 0.17	0.1516
LV posterior wall systolic, mm	2.8 ± 0.14	2.9 ± 0.09	0.3026
LV posterior wall diastolic, mm	1.6 ± 0.05	1.6 ± 0.11	0.9937
Key: BP, blood pressure; LV, left ventricular, MABP, mean arterial blood pressure; RUPP, reduced uterine perfusion pressure.			
Unpaired student's t-test, *p < 0.05, ***p < 0.001.			

To investigate cardiac health in the RUPP model, echocardiography was performed. No statistically significant differences in stroke volume, cardiac output, ejection fraction or fractional shortening were observed between sham or RUPP rats (Table 1). The RUPP hearts had significantly higher corrected LV mass. Once isolated, the hearts were weighed and RUPP rat hearts were found to be significantly heavier than the controls (Table 1). However, as maternal body weights were also significantly heavier in RUPP rats compared to sham controls, this did not translate to a significant difference between the wet heart: body weight ratio of each group (Table 1).

RUPP induces fibrosis and increased FKBPL in rat hearts

Picrosirius red staining of collagen I/III fibres revealed a statistically significant increase in collagen deposition in RUPP hearts compared to control (Fig. 1A-B), indicating the development of cardiac fibrosis (sham 9.9 ± 0.8 vs RUPP 18.7 ± 0.9, %; n = 6, p < 0.001). Additionally, BNP, a well-established marker of cardiac hypertrophy and diastolic dysfunction[33], was analysed by ELISA using the rat heart protein lysates, showing a statistically significant increase in BNP protein expression in RUPP hearts compared to sham controls (sham 4.1 ± 1.6 vs RUPP 11.8 ± 2.1, ng/µl, n = 6, p = 0.01, Fig. 1C).

RT-qPCR showed a significant increase in the mRNA expression of *Fkbpl* in RUPP rat hearts (sham 1.14 ± 0.24 vs RUPP 2.57 ± 0.6, fold change, n = 6, p = 0.03, Fig. 2A). Given the FKBPL protein is prone to post-translational modifications, this

difference in expression needed to be confirmed at the protein level. Indirect ELISA revealed a statistically significant increase in FKBPL protein concentration in RUPP hearts (sham 5365 ± 626.7 vs RUPP 9263 ± 1112, ng/ml, p = 0.007, Fig. 2B). Nevertheless, there were no statistically significant differences in the mRNA expression of *Flt1* (sham 1.01 ± 0.05 vs RUPP 0.9 ± 0.08, n ≥ 6, p > 0.05, Fig. 2C) or *Vegfa* (sham 1.01 ± 0.06 vs RUPP 1.36 ± 0.2, n ≥ 6, p > 0.05, Fig. 2D) between the hearts of RUPP and sham rats. Similarly, no significant differences between the mRNA expression of *Icam1* or *Vcam1* in the hearts of sham or RUPP rats (Additional File 1, Supplementary Fig. 1).

RUPP procedure leads to fibrosis and decreased Flt1 in rat placentae

Picrosirius red staining of collagen fibres I/III revealed a statistically significant increase in collagen deposition in RUPP placentae, indicating the presence of some level of placental fibrosis (sham 1.6 ± 0.2 vs RUPP 2.4 ± 0.3, %, n = 7, p = 0.03; Fig. 3.A-B).

Similar to the rat hearts, total RNA was isolated and analysed by RT-qPCR to determine any changes to mRNA expression levels of *Icam1*, *Vcam1*, *Flt1* and *Vegfa*. There was, however, a decrease in expression of *Flt1* mRNA in RUPP placental tissue (sham 1.016 ± 0.04 vs RUPP 0.85 ± 0.07, fold change, n = 7, p = 0.048, Fig. 3C). There was no significant difference in the *Vegfa* mRNA levels in placentae between the Sham and RUPP rats (sham 1.029 ± 0.085 vs RUPP 0.897 ± 0.091, n = 7, p = 0.189, Fig. 3D). As shown in Supplementary Fig. 2, there was no statistically significant difference in expression of *Icam1* or *Vcam1* mRNA between the sham or RUPP groups.

Increased glomerular size is observed in RUPP kidneys

H&E staining of rat kidneys was performed to visualise tissue morphology. The area of 50 glomeruli within kidney sections was measured per animal using Zen Lite (v3.2). The mean of these results demonstrated a significant increase in the overall size of the glomeruli within the Bowman's capsules' of RUPP rats compared to sham controls (sham 4355 ± 103.5 vs RUPP 4935 ± 204.6, μm^2, n = 7, p = 0.03; Fig. 4).

Signs of potential liver inflammation are observed in RUPP livers

Given preeclampsia often manifests in liver dysfunction, we performed histological analysis of rat livers. H&E analysis of rat liver tissue (presented in Supplementary Fig. 3) revealed an increase in the population of small cells (5–15μm^2) in RUPP rats, indicative of inflammatory cells. Picrosirius red staining revealed no significant increase in collagen I/III fibres (Supplementary Fig. 4).

Plasma samples from women with preeclampsia led to increased FKBPL expression in cardiac spheroids.

Human 3D cardiac spheroids were generated by co-culturing cardiac fibroblasts and endothelial cells to analyse FKBPL and CD31 protein expression following treatment with normotensive (healthy), EOPE and LOPE human plasma samples. Following incubation in human plasma, cardiac spheroids were fixed and probed for immunofluorescent visualisation of FKBPL and CD31 proteins (Fig. 5). Semi-quantitative protein expression was measured by quantifying immunofluorescent intensity of stained spheroids. This data demonstrated a trend towards increased FKBPL expression in EOPE-treated spheroids compared to normotensive control plasma (control 1.00 ± 0.13 vs EOPE 1.43 ± 0.125, n = 3, p = 0.06, Fig. 6A) and a significant increase in the expression of FKBPL in LOPE-treated spheroids compared to normotensive control plasma (control 1.00 ± 0.13 vs LOPE 1.58 ± 0.05; p = 0.03; Fig. 6A). There was a slight trend towards an increase in CD31 expression in EOPE-treated spheroids compared to control however this was not statistically significant (control 1.00 ± 0.07 vs EOPE 1.34 ± 0.14, n = 3, p = 0.18, Fig. 6B). There was no significant difference in CD31 protein expression between LOPE-treated spheroids and healthy control (control 1.00 ± 0.07 vs LOPE 1.05 ± 0.129; p = 0.95; Fig. 6B) after treatment with

patient plasma samples. No significance was determined between EOPE- and LOPE- treated cardiac spheroids in terms of FKBPL or CD31 expression.

Discussion

Animal models of preeclampsia have been difficult to establish, primarily due to the fact that preeclampsia does not spontaneously occur in most species other than humans and the presence of inter-species variations [34]. The most reliable animal model of preeclampsia is the surgically-induced RUPP model in rats or mice. This model has been shown to induce hypertension[35], proteinuria[35], renal dysfunction[35, 36], an anti-angiogenic state[37], abnormal immune responses[38–40], vasoconstriction[41], oxidative stress[42], cardiac dysfunction[43] and IUGR [44, 45] like that of preeclampsia in humans. However, the cardiovascular dysfunction particularly in terms of heart health has not been extensively studied in this model of preeclampsia before[46]. Although there is substantial evidence published exploring this model's reflection of human features of preeclampsia, we aimed to confirm the cardiovascular phenotype in RUPP rats and to determine the presence of altered FKBPL expression. This is the first study that explores the role of this novel anti-angiogenic protein in cardiovascular features of preeclampsia.

In this study, surgically reduced perfusion to the uterus in pregnant rats resulted in anatomical and physiological alterations to maternal hearts, placentae and kidneys with a number of features of preeclampsia being demonstrated. Given the well-established association between preeclampsia and increased risk of developing future CVD[47], this is an important aspect in modelling the manifestation of preeclampsia. In fact, recently published results describe the overlapping mechanisms between preeclampsia and future cardiovascular disease with angiogenesis- and inflammatory-related pathways playing a key role[15].

A significant increase in systolic, diastolic and mean arterial blood pressure confirmed that the RUPP procedure had been successful and increased heart rate with LV hypertrophy were evident, as determined by echocardiography. In our model, we did not apply too much pressure on the uterine clips and hence did not observe significant changes in the embryo weight or number in the RUPP rats, suggesting that it may be more representative of a LOPE phenotype. LOPE is diagnosed from 34 weeks of gestation, it is a less understood phenotype of preeclampsia, likely occurring secondary to maternal microvascular diseases, reflective of underlying vascular dysfunction. It seems to develop due to maternal inability to meet metabolic and cardiovascular demands of the growing foetus. On the other hand, EOPE is usually diagnosed before 34 weeks' of gestation and associated with foetal growth restriction as well as inadequate or incomplete trophoblast invasion of spiral uterine arteries, often implicating placenta as the root cause[17]. Nevertheless, our analysis of placental collagen deposition found RUPP placenta to be more fibrotic compared to sham controls. Placental fibrosis has been found to occur in placentae of women with preeclampsia compared to normotensive controls[48]. Additional quantification of fibrotic factors including connective tissue growth factor (CTGF) or fibronectin in these placentae could aid in determining levels of fibrosis. Of note, placental fibrosis is a prominent feature of preeclamptic placentae and has been shown to be associated with activation of stromal fibroblasts via the TGF-β1 signalling pathway[48]. Reduced angiogenesis as depicted by decreased *Flt1* expression further support this finding.

Further, given that preeclampsia is frequently associated with altered renal function and histology, RUPP and sham kidneys were inspected for altered tissue morphology showing that glomeruli in RUPP samples had a significantly larger surface area. While the RUPP model has not yet been described as displaying glomerular endotheliosis, a characteristic feature of preeclampsia[49, 50], some changes to kidney tissue were previously noted. Nevertheless, this measurement is limited to 2-dimensional analysis rather than a 3-dimensional measurement of each glomerular structure and the characteristic endothelial swelling was not observed, our data suggests glomerular endotheliosis may be present in RUPP rats, which has previously been observed in an sFlt-1 administration model of preeclampsia in rats[51]. Electron microscopy or glomerular filtration rate would be important tools to measure this in future experiments. Moreover, previous

studies have demonstrated an increase in proteinuria and a decrease in glomerular filtration rate following the RUPP procedure, with the latter lasting up to 8 weeks postpartum[52, 53].

In relation to cardiovascular health in the RUPP model, picrosirius red staining of RUPP hearts suggests the presence of cardiac fibrosis compared to sham controls, which is consistent with the preeclampsia phenotype and increased risk of CVD including cardiac fibrosis, later in life[54–56]. These results are also consistent with another study characterising the cardiac effects of RUPP in rats that showed a significant increase in collagen I/III fibrotic markers in RUPP hearts [57]; these effects have been shown to be reversed post a RUPP pregnancy[53]. BNP is released from the cardiac ventricles in response to diastolic and systolic dysfunction, which places additional stress on the heart walls[58, 59]. We have noted a significant increase in cardiac levels of BNP, which is supported by other studies' findings in preeclampsia models [57, 60].

In addition to cardiac fibrosis, FKBPL was significantly increased at the mRNA level as a result of RUPP procedure. However, FKBPL is a chaperone protein and prone to post-transcriptional modification so quantification of its expression at the protein level is more informative[61]. Therefore, ELISA was performed on rat heart protein lysates and indeed confirmed an increase in FKBPL protein levels in RUPP hearts, suggesting that FKBPL could be a novel mechanism of cardiovascular damage in preeclampsia. Further, recent data from our group has shown that FKBPL is increased as a result of cardiac fibrosis and TGF-β stimulation in cardiac fibroblasts[62]. FKBPL is also increased in plasma and placentae from women with preeclampsia[19], and in people with CVD[20].

The use of an appropriate 3D cell culture model to study the effects of secreted placental factors on cardiac heart cells would enable a deeper exploration of the cardiac effects of preeclampsia. While traditional 2D cell culture methods are limited in their ability to recapitulate the cellular structure and function within a tissue, three-dimensional (3D) cell culture methods with polymer-containing extracellular matrix (ECM), provide a 3D cell architecture allowing interaction in all spatial dimensions with both other cells and their environment. This allows for fine-tuning of the microenvironment by modifying properties including elasticity, stiffness, conductivity and porosity[63].

FKBPL in the cardiac spheroid model was evaluated to determine its role in a human models of cardiac spheroids in the presence of plasma from patients with EOPE, LOPE and healthy controls. CD31 is a marker of endothelial cells and as such evaluation of this marker was used to interpret FKBPL expression in the context of endothelial cell health within cardiac spheroids. Analysis determined that FKBPL expression was elevated in LOPE-treated spheroids when compared to healthy controls. We also noted a trend of increased FKBPL expression in EOPE-treated spheroids compared to control, though this was not significant likely due to small sample size. This is in alignment with studies performed by Gonzalez-Quinero *et al.* showing that endothelial microparticles were over expressed in women with preeclampsia compared to women with healthy pregnancies and those presenting with gestational hypertension[64]. Therefore, it appears that circulating factors in maternal plasma during preeclampsia may induce an overexpression of FKBPL in cardiac fibroblast and/or endothelial cells. While this did not induce a notable change in CD31 expression, this model could be used to further study the mechanism of this effect. Adding cardiomyocytes to the co-culture in a 2:1:1 ratio with the fibroblasts and endothelial cells used has been shown to produce a vascularised cardiac spheroid suspension, which have the potential to produce a more representative model of cardiac health in preeclampsia[65].

Perspectives and Significance

This is the first study that implicates FKBPL as a novel anti-angiogenic mechanism in cardiovascular dysfunction as a result of preeclampsia that could be explored in the future for better understanding of the association between preeclampsia and future CVD risk. Furthermore, our study demonstrated that preeclampsia could induce cardiac fibrosis and diastolic dysfunction in association with increased FKBPL levels. This knowledge is important for developing future monitoring and treatment strategies to prevent heart disease in women during and post preeclampsia.

Conclusions

In our RUPP model cardiac, renal and placental features in pregnant rats are reflective of that of preeclampsia in humans, especially those of LOPE. Furthermore, we demonstrate, for the first time, that FKBPL is overexpressed in the hearts of RUPP rats and cardiac spheroids treated with plasma from women with preeclampsia, supporting our hypothesis that this novel anti-angiogenic mechanism may be important in cardiovascular dysfunction associated with preeclampsia.

Declarations

Ethics approval and consent to participate

Animal ethics for this project was obtained from the Northern Sydney Local Health District Animal Ethics Committee at the Kolling Institute and was carried out in according to the Australian code for the care and use of animals for scientific purposes. Human sample collection was approved by the local institutional review boards and written informed consent was obtained from all participants as per the principles outlined in the Declaration of Helsinki.

Consent for publication

All authors have consented to the publication of this manuscript.

Availability of data and materials

The datasets generated and analyzed in the current project are available from the corresponding author upon reasonable request.

Competing interests

The authors declare that they have no financial competing interests.

Funding

Funding for this project was obtain from the Faculty of Science, University of Technology Sydney.

Authors' contributions

LM conceptualised the project, carried out experiments, analysed and interpreted the data and edited manuscript. CR carried out experiments, analysed and interpreted the data and wrote the manuscript. KB, KM and CG designed and performed experiments, analysed and interpreted the data. KS, MC, SG, CR, CLCM, CE carried out experiments and/or data analysis and interpretation. VN, NKO, ZM, MS, ZC coordinated and collected human plasma samples from women with and without preeclampsia and provided clinical data. All authors reviewed and approved the final manuscript.

Acknowledgments

The authors acknowledge the use of the equipment ZEISS Axio Scan.Z1 in the Microbial Imaging Facility at the i3 institute in the Faculty of Science, the University of Technology Sydney. We would like to thank A/Prof Louise Cole for her assistance in providing training to CR.

References

1. Say L, Chou D, Gemmill A, Tunçalp Ö, Moller A-B, Daniels J, et al. Global causes of maternal death: a WHO systematic analysis. Lancet Glob Heal. 2014;2:e323-33. doi:10.1016/S2214-109X(14)70227-X.

2. Steegers EA, von Dadelszen P, Duvekot JJ, Pijnenborg R. Pre-eclampsia. Lancet. 2010;376:631–44. doi:10.1016/S0140-6736(10)60279-6.
3. Tranquilli AL, Dekker G, Magee L, Roberts J, Sibai BM, Steyn W, et al. The classification, diagnosis and management of the hypertensive disorders of pregnancy: A revised statement from the ISSHP. Pregnancy Hypertens An Int J Women's Cardiovasc Heal. 2014;4:97–104. doi:10.1016/J.PREGHY.2014.02.001.
4. Henderson JT, Whitlock EP, O'Connor E, Senger CA, Thompson JH, Rowland MG. Low-Dose Aspirin for Prevention of Morbidity and Mortality From Preeclampsia: A Systematic Evidence Review for the U.S. Preventive Services Task Force. Ann Intern Med. 2014;160:695–703. doi:10.7326/M13-2844.
5. Rolnik DL, Wright D, Poon LC, O'Gorman N, Syngelaki A, de Paco Matallana C, et al. Aspirin versus Placebo in Pregnancies at High Risk for Preterm Preeclampsia. N Engl J Med. 2017;377:613–22.
6. Everett TR, Wilkinson IB, Lees CC. Drug development in preeclampsia: a 'no go' area? J Matern Neonatal Med. 2012;25:50–2. doi:10.3109/14767058.2011.557791.
7. Lykke JA, Langhoff-Roos J, Sibai BM, Funai EF, Triche EW, Paidas MJ. Hypertensive Pregnancy Disorders and Subsequent Cardiovascular Morbidity and Type 2 Diabetes Mellitus in the Mother. Hypertension. 2009;53:944–51.
8. Manten GTR, Sikkema MJ, Voorbij HAM, Visser GHA, Bruinse HW, Franx A. Risk Factors for Cardiovascular Disease in Women with a History of Pregnancy Complicated by Preeclampsia or Intrauterine Growth Restriction. Hypertens Pregnancy. 2007;26:39–50. doi:10.1080/10641950601146574.
9. Libby G, Murphy DJ, McEwan NF, Greene SA, Forsyth JS, Chien PW, et al. Pre-eclampsia and the later development of type 2 diabetes in mothers and their children: an intergenerational study from the Walker cohort. Diabetologia. 2007;50:523–30. doi:10.1007/s00125-006-0558-z.
10. Davis EF, Lazdam M, Lewandowski AJ, Worton SA, Kelly B, Kenworthy Y, et al. Cardiovascular Risk Factors in Children and Young Adults Born to Preeclamptic Pregnancies: A Systematic Review. Pediatrics. 2012;129:e1552–e1561. doi:10.1542/peds.2011-3093.
11. Alsnes I V, Vatten LJ, Fraser A, Bjørngaard JH, Rich-Edwards J, Romundstad PR, et al. Hypertension in Pregnancy and Offspring Cardiovascular Risk in Young Adulthood. Hypertension. 2017;69:591–8.
12. Roth H, LeMarquand G, Henry A, Homer C. Assessing Knowledge Gaps of Women and Healthcare Providers Concerning Cardiovascular Risk After Hypertensive Disorders of Pregnancy-A Scoping Review. Frontiers in cardiovascular medicine. 2019;6:178.
13. Veerbeek JHW, Hermes W, Breimer AY, van Rijn BB, Koenen S V, Mol BW, et al. Cardiovascular disease risk factors after early-onset preeclampsia, late-onset preeclampsia, and pregnancy-induced hypertension. Hypertens (Dallas, Tex 1979). 2015;65:600–6.
14. Lopez-Campos G, Bonner E, McClements L. An Integrative Biomedical Informatics Approach to Elucidate the Similarities Between Pre-Eclampsia and Hypertension. Stud Health Technol Inform. 2019;264:988–92.
15. Suvakov S, Bonner E, Nikolic V, Jerotic D, Simic TP, Garovic VD, et al. Overlapping pathogenic signalling pathways and biomarkers in preeclampsia and cardiovascular disease. Pregnancy Hypertens. 2020;20:131–6. doi:https://doi.org/10.1016/j.preghy.2020.03.011.
16. Staff AC. The two-stage placental model of preeclampsia: An update. J Reprod Immunol. 2019;134–135:1–10. doi:10.1016/J.JRI.2019.07.004.
17. Burton GJ, Redman CW, Roberts JM, Moffett A. Pre-eclampsia: pathophysiology and clinical implications. BMJ. 2019;366. doi:10.1136/bmj.l2381.
18. Walshe TE, Dole VS, Maharaj ASR, Patten IS, Wagner DD, D'Amore PA. Inhibition of VEGF or TGF-β Signaling Activates Endothelium and Increases Leukocyte Rolling. Arterioscler Thromb Vasc Biol. 2009;29:1185–92.
19. Todd N, McNally R, Alqudah A, Jerotic D, Suvakov S, Obradovic D, et al. Role of a novel angiogenesis FKBPL-CD44 pathway in preeclampsia risk stratification and mesenchymal stem cell treatment. J Clin Endocrinol Metab. 2020.

20. Andrzej S Januszewski, Chris J Watson, Vikki O'Neill, Kenneth McDonald, Mark Ledwidge, Tracy Robson, Alicia J Jenkins ACKM and LM. FKBPL is associated with metabolic parameters and is a novel determinant of cardiovascular disease. Sci Rep. 2020;Accepted.
21. Jascur T, Brickner H, Salles-Passador I, Barbier V, Khissiin] A [El, Smith B, et al. Regulation of p21WAF1/CIP1 Stability by WISp39, a Hsp90 Binding TPR Protein. Mol Cell. 2005;17:237–49. doi:https://doi.org/10.1016/j.molcel.2004.11.049.
22. McKeen HD, McAlpine K, Valentine A, Quinn DJ, McClelland K, Byrne C, et al. A Novel FK506-Like Binding Protein Interacts with the Glucocorticoid Receptor and Regulates Steroid Receptor Signaling. Endocrinology. 2008;149:5724–34. doi:10.1210/en.2008-0168.
23. Sunnotel O, Hiripi L, Lagan K, McDaid J, León J, Miyagawa Y, et al. Alterations in the steroid hormone receptor co-chaperone FKBPL are associated with male infertility: a case-control study. Reprod Biol Endocrinol. 2010;8:22.
24. Yakkundi A, Bennett R, Hernández-Negrete I, Delalande J-M, Hanna M, Lyubomska O, et al. FKBPL is a critical antiangiogenic regulator of developmental and pathological angiogenesis. Arterioscler Thromb Vasc Biol. 2015;35:845–54.
25. McClements L, Annett S, Yakkundi A, O'Rourke M, Valentine A, Moustafa N, et al. FKBPL and its peptide derivatives inhibit endocrine therapy resistant cancer stem cells and breast cancer metastasis by downregulating DLL4 and Notch4. BMC Cancer. 2019;19:351. doi:10.1186/s12885-019-5500-0.
26. Annett S, Moore G, Short A, Marshall A, McCrudden C, Yakkundi A, et al. FKBPL-based peptide, ALM201, targets angiogenesis and cancer stem cells in ovarian cancer. Br J Cancer. 2020;122:361–71. doi:10.1038/s41416-019-0649-5.
27. Yakkundi A, McCallum L, O'Kane A, Dyer H, Worthington J, McKeen HD, et al. The anti-migratory effects of FKBPL and its peptide derivative, AD-01: regulation of CD44 and the cytoskeletal pathway. PLoS One. 2013;8:e55075.
28. Valentine A, O'Rourke M, Yakkundi A, Worthington J, Hookham M, Bicknell R, et al. FKBPL and Peptide Derivatives: Novel Biological Agents That Inhibit Angiogenesis by a CD44-Dependent Mechanism. Clin Cancer Res. 2011;17:1044–56.
29. Li J, LaMarca B, Reckelhoff JF. A model of preeclampsia in rats: the reduced uterine perfusion pressure (RUPP) model. Am J Physiol Heart Circ Physiol. 2012;303:H1-8.
30. Morillon A-C, Williamson RD, Baker PN, Kell DB, Kenny LC, English JA, et al. Effect of L-Ergothioneine on the metabolic plasma profile of the RUPP rat model of pre-eclampsia. PLoS One. 2020;15:e0230977.
31. Polonchuk L, Chabria M, Badi L, Hoflack J-C, Figtree G, Davies MJ, et al. Cardiac spheroids as promising in vitro models to study the human heart microenvironment. Sci Rep. 2017;7:7005.
32. ACOG Practice Bulletin No. 202: Gestational Hypertension and Preeclampsia. Obstet Gynecol. 2019;133:e1–25.
33. Ledwidge M, Gallagher J, Conlon C, Tallon E, O'Connell E, Dawkins I, et al. Natriuretic Peptide–Based Screening and Collaborative Care for Heart Failure. JAMA. 2013;310:66.
34. Turbeville HR, Sasser JM. Preeclampsia beyond pregnancy:Long-term consequences for mother and child. Am J Physiol Physiol. 0. doi:10.1152/ajprenal.00071.2020.
35. Alexander BT, Kassab SE, Miller MT, Abram SR, Reckelhoff JF, Bennett WA, et al. Reduced Uterine Perfusion Pressure During Pregnancy in the Rat Is Associated With Increases in Arterial Pressure and Changes in Renal Nitric Oxide. Hypertension. 2001;37:1191–5.
36. Sholook MM, Gilbert JS, Sedeek MH, Huang M, Hester RL, Granger JP. Systemic hemodynamic and regional blood flow changes in response to chronic reductions in uterine perfusion pressure in pregnant rats. Am J Physiol Circ Physiol. 2007;293:H2080–4. doi:10.1152/ajpheart.00667.2007.
37. Gilbert JS, Babcock SA, Granger JP. Hypertension Produced by Reduced Uterine Perfusion in Pregnant Rats Is Associated With Increased Soluble Fms-Like Tyrosine Kinase-1 Expression. Hypertension. 2007;50:1142–7.

38. LaMarca BBD, Bennett WA, Alexander BT, Cockrell K, Granger JP. Hypertension Produced by Reductions in Uterine Perfusion in the Pregnant Rat. Hypertension. 2005;46:1022–5.
39. Gadonski G, LaMarca BBD, Sullivan E, Bennett W, Chandler D, Granger JP. Hypertension Produced by Reductions in Uterine Perfusion in the Pregnant Rat. Hypertension. 2006;48:711–6.
40. Wallace K, Richards S, Dhillon P, Weimer A, Edholm E, Bengten E, et al. $CD4^+$ T-Helper Cells Stimulated in Response to Placental Ischemia Mediate Hypertension During Pregnancy. Hypertension. 2011;57:949–55.
41. Crews JK, Herrington JN, Granger JP, Khalil RA. Decreased Endothelium-Dependent Vascular Relaxation During Reduction of Uterine Perfusion Pressure in Pregnant Rat. Hypertension. 2000;35:367–72.
42. Sedeek M, Gilbert JS, LaMarca BB, Sholook M, Chandler DL, Wang Y, et al. Role of Reactive Oxygen Species in Hypertension Produced by Reduced Uterine Perfusion in Pregnant Rats. Am J Hypertens. 2008;21:1152–6. doi:10.1038/ajh.2008.239.
43. Bakrania BA, Hall ME, Shahul S, Granger JP. The Reduced Uterine Perfusion Pressure (RUPP) rat model of preeclampsia exhibits impaired systolic function and global longitudinal strain during pregnancy. Pregnancy Hypertens. 2019;18:169–72. doi:https://doi.org/10.1016/j.preghy.2019.10.001.
44. Alexander BT. Placental Insufficiency Leads to Development of Hypertension in Growth-Restricted Offspring. Hypertension. 2003;41:457–62.
45. Kupferminc MJ, Peaceman AM, Wigton TR, Rehnberg KA, Socol ML. Tumor necrosis factor-α is elevated in plasma and amniotic fluid of patients with severe preeclampsia. Am J Obstet Gynecol. 1994;170:1752–9. doi:10.1016/S0002-9378(12)91845-1.
46. Gatford KL, Andraweera PH, Roberts CT, Care AS. Animal Models of Preeclampsia. Hypertens AHA. 2020;75:10.1161/HYPERTENSIONAHA.119.14598.
47. Irgens HU, Roberts JM, Reisæter L, Irgens LM, Lie RT. Long term mortality of mothers and fathers after pre-eclampsia: population based cohort studyPre-eclampsia and cardiovascular disease later in life: who is at risk? BMJ. 2001;323:1213–7. doi:10.1136/bmj.323.7323.1213.
48. Ohmaru-Nakanishi T, Asanoma K, Fujikawa M, Fujita Y, Yagi H, Onoyama I, et al. Fibrosis in Preeclamptic Placentas Is Associated with Stromal Fibroblasts Activated by the Transforming Growth Factor-B1 Signaling Pathway. Am J Pathol. 2018;188:683–95. doi:10.1016/j.ajpath.2017.11.008.
49. Strevens H, Wide-Swensson D, Hansen A, Horn T, Ingemarsson I, Larsen S, et al. Glomerular endotheliosis in normal pregnancy and pre-eclampsia. BJOG An Int J Obstet Gynaecol. 2003;110:831–6. doi:10.1111/j.1471-0528.2003.02162.x.
50. Stillman IE, Karumanchi SA. The Glomerular Injury of Preeclampsia. J Am Soc Nephrol. 2007;18:2281–4. doi:10.1681/ASN.2007020255.
51. Maynard SE, Min J-Y, Merchan J, Lim K-H, Li J, Mondal S, et al. Excess placental soluble fms-like tyrosine kinase 1 (sFlt1) may contribute to endothelial dysfunction, hypertension, and proteinuria in preeclampsia. J Clin Invest. 2003;111:649–58.
52. Tian X, Ma S, Wang Y, Hou L, Shi Y, Yao M, et al. Effects of Placental Ischemia Are Attenuated by 1,25-Dihydroxyvitamin D Treatment and Associated with Reduced Apoptosis and Increased Autophagy. DNA Cell Biol. 2016;35:59–70.
53. Paauw ND, Joles JA, Spradley FT, Bakrania B, Zsengeller ZK, Franx A, et al. Exposure to placental ischemia impairs postpartum maternal renal and cardiac function in rats. Am J Physiol Regul Integr Comp Physiol. 2017;312:R664–70.
54. Cong J, Fan T, Yang X, Shen J, Cheng G, Zhang Z. Maternal cardiac remodeling and dysfunction in preeclampsia: a three-dimensional speckle-tracking echocardiography study. Int J Cardiovasc Imaging. 2015;31:1361–8. doi:10.1007/s10554-015-0694-y.

55. Scantlebury DC, Kane GC, Wiste HJ, Bailey KR, Turner ST, Arnett DK, et al. Left ventricular hypertrophy after hypertensive pregnancy disorders. Heart. 2015;101:1584–90.
56. Bokslag A, Franssen C, Alma LJ, Kovacevic I, Kesteren F van, Teunissen PW, et al. Early-onset preeclampsia predisposes to preclinical diastolic left ventricular dysfunction in the fifth decade of life: An observational study. PLoS One. 2018;13:e0198908.
57. Gutkowska J, Granger JP, Lamarca BB, Danalache BA, Wang D, Jankowski M. Changes in cardiac structure in hypertension produced by placental ischemia in pregnant rats: effect of tumor necrosis factor blockade. J Hypertens. 2011;29. https://journals.lww.com/jhypertension/Fulltext/2011/06000/Changes_in_cardiac_structure_in_hypertension.25.aspx.
58. Ambrosi P, Oddoze C, Habib G. Utility of B-natriuretic peptide in detecting diastolic dysfunction: comparison with Doppler velocity recordings. Circulation. 2002;106:e70.
59. McDonagh TA, Robb SD, Murdoch DR, Morton JJ, Ford I, Morrison CE, et al. Biochemical detection of left-ventricular systolic dysfunction. Lancet (London, England). 1998;351:9–13.
60. Ding L, Bai C, Liu Y. Interleukin-6 contributes to myocardial damage in pregnant rats with reduced uterine perfusion pressure. Brazilian J Med Biol Res = Rev Bras Pesqui medicas e Biol. 2018;51:e6921.
61. Mcclements L, Annett S, Yakkundi A, Robson T. The Role of Peptidyl Prolyl Isomerases in Aging and Vascular Diseases. Curr Mol Pharmacol. 2015;9.
62. McClements L, Rayner B, Alqudah A, Grieve D, Robson T. FKBPL, a novel player in cardiac ischaemia and fibrosis. J Mol Cell Cardiol. 2020;140:5. doi:10.1016/j.yjmcc.2019.11.008.
63. Vunjak Novakovic G, Eschenhagen T, Mummery C. Myocardial tissue engineering: in vitro models. Cold Spring Harb Perspect Med. 2014;4.
64. González-Quintero VH, Smarkusky LP, Jiménez JJ, Mauro LM, Jy W, Hortsman LL, et al. Elevated plasma endothelial microparticles: preeclampsia versus gestational hypertension. Am J Obstet Gynecol. 2004;191:1418–24.
65. Figtree GA, Bubb KJ, Tang O, Kizana E, Gentile C. Vascularized Cardiac Spheroids as Novel 3D in vitro Models to Study Cardiac Fibrosis. Cells Tissues Organs. 2017;204:191–8.

Figures

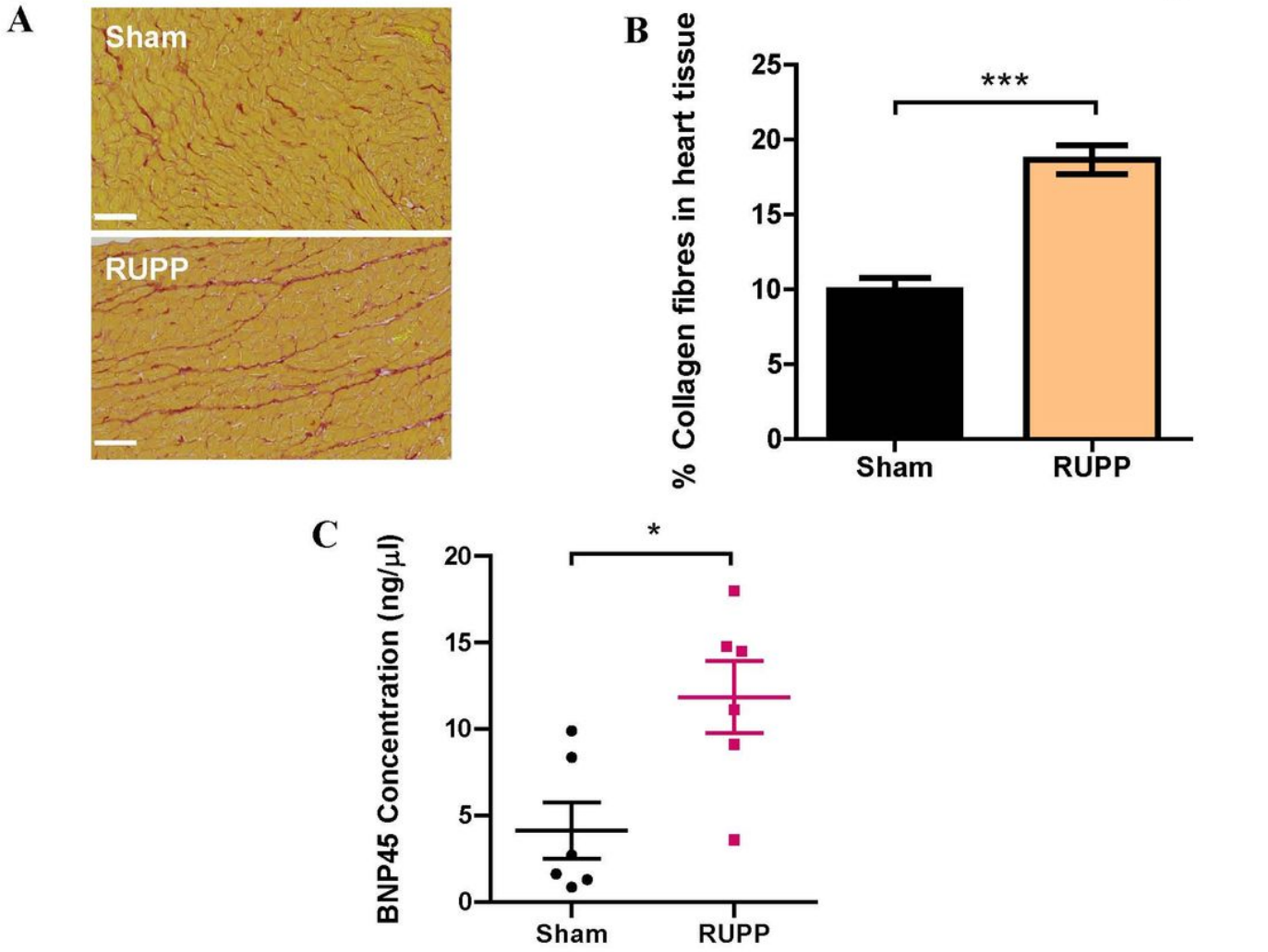

Figure 1

RUPP surgery increases collagen deposition in rat hearts. (A-B) Paraffin embedded rat hearts were sectioned at 10µm thickness and stained with picrosirius red staining to visualise collagen I/III (red) and muscle cell cytoplasm (yellow) in sham and RUPP rats. Scalebar = 50µm. Images taken at 5x using an Axioscan microscope were analysed for percentage area stained red to quantify collagen deposition as an indicator of cardiac fibrosis. (C) Rat heart protein isolated by homogenisation with RIPA lysis buffer was quantified by indirect ELISA against known standards to quantify protein concentration of BNP45. Data points are expressed as mean percentage ± SEM; n≥6, unpaired student's t-test; *p<0.05, ***p<0.0001.

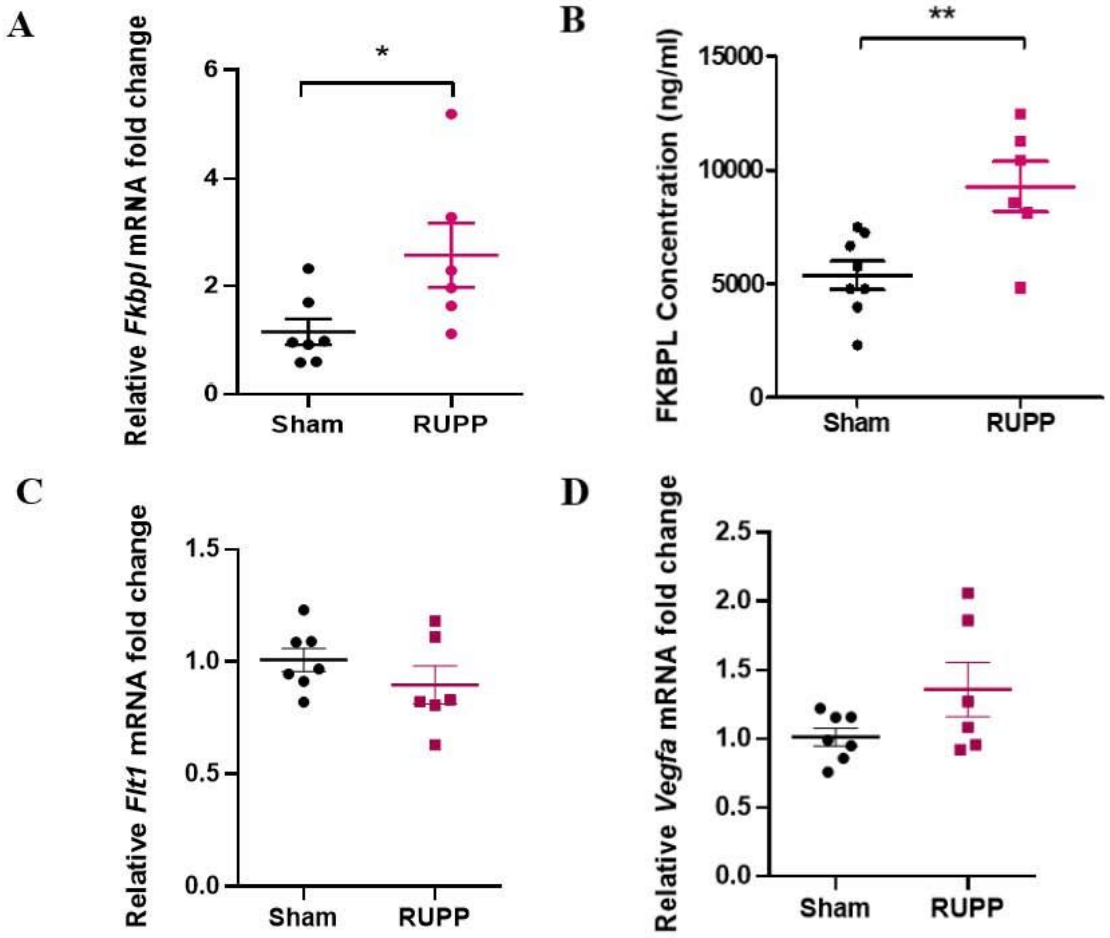

Figure 2

RUPP hearts express higher mRNA and protein levels of FKBPL. Total RNA extracted from rat hearts by TRIsure reagent was analysed by RT-qPCR to determine mRNA expression levels of Fkbpl, Flt1 and Vegfa. Relative mRNA expression of (A) Fkbpl comparing sham and RUPP hearts. Data presented as mean ± SEM; n≥6; Mann-Whitney t-test; *p<0.05. Fkbpl expression was verified at the protein level by enzyme-linked immunosorbent assay (ELISA) and concentration calculated against a known standard (B). Data presented as mean ± SEM; n≥6; unpaired Student's t-test, **p<0.01 (C) Relative Flt1 mRNA and (D) Vegfa mRNA levels comparing sham and RUPP rat groups. Data presented as mean fold change ± SEM; n≥6; Mann-Whitney t-test.

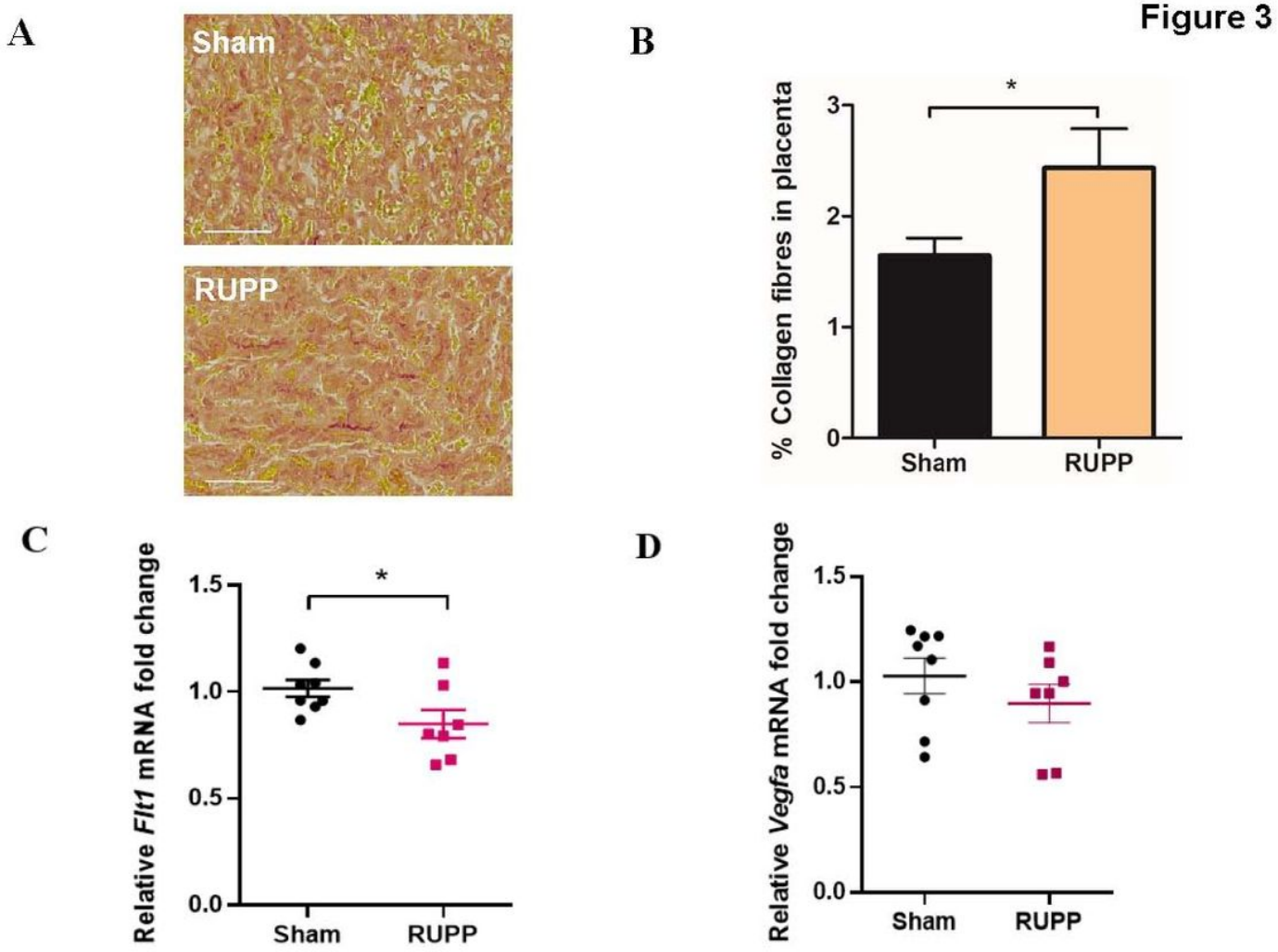

Figure 3

RUPP rats have increased collagen deposition and decreased Flt1 mRNA expression in their placentae. (A) Paraffin embedded rat placentae were sectioned at 10μm thickness and stained by picrosirius red staining to visualise collagen I/III fibres (red) in sham and RUPP hearts. Scalebar = 100μm. (B) Images of picrosirius red-stained tissue were taken at 5x using an Axioscan microscope and analysed for percentage of area stained red to quantify collagen deposition as an indicator of placental fibrosis. Data points are mean ± SEM; n=7, unpaired student's t-test; *<0.05. RNA extracted from rat placentae by TRIsure reagent was analysed by RT-qPCR to determine mRNA expression levels of (C) Flt1 and (D) Vegfa. Data presented as mean fold change ± SEM; n=7; Mann-Whitney t-test; *p<0.05.

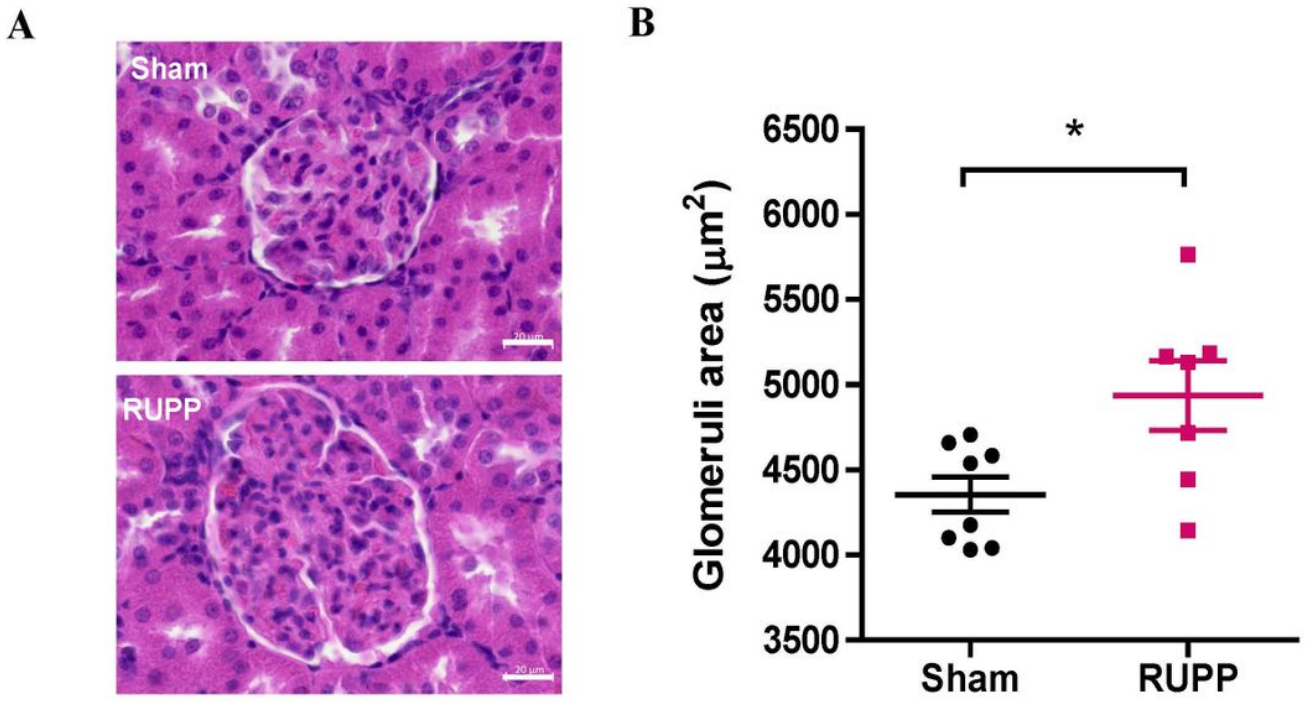

Figure 4

RUPP rats present with larger glomeruli in rat kidneys. Paraffin-embedded rat kidneys were cut at 10 μm sections and stained with H&E staining to visualize tissue morphology. (A) Images of entire tissue sections were taken at 4x, 10x and 20x objective using an Axioscan microscope to produce virtual slides of sham and RUPP kidneys. Scalebar =20μm. (B) Average glomerular area was measured at a 20x magnification using ZEN Lite 3.2 software. Data plotted as mean ± SEM; n=7; unpaired student's t-test, *<0.05.

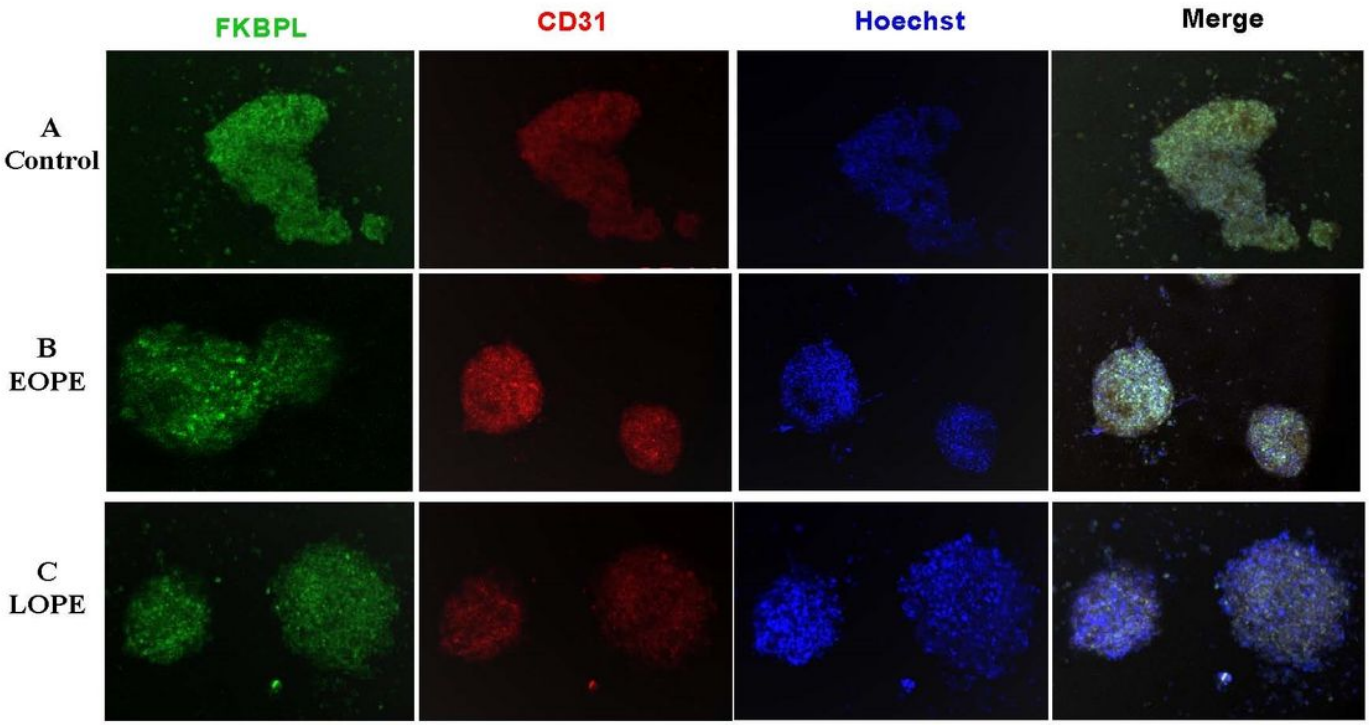

Figure 5

Immunofluorescent images of cardiac spheroids treated with plasma samples from healthy control, early-onset and late-onset preeclampsia patients. Cardiac spheroids were generated in hanging droplets by co-culturing primary human cardiac fibroblast cells (HCFs) and human coronary artery endothelial cells (HCAECs) in a 1:1 ratio. Following formation of 3D structures, the spheroids were treated with human plasma samples from women with or without preeclampsia. After plasma treatment, spheroids were fixated and permeabilised prior to labelled with antibodies (FKBPL, CD31) and fluorescent stain (Hoechst). (A) Spheroids treated with plasma from normotensive control pregnancies. (B) Spheroids treated early-onset preeclampsia (EOPE) patient plasma. (C) Spheroids treated with late-onset preeclampsia (LOPE) patient plasma.

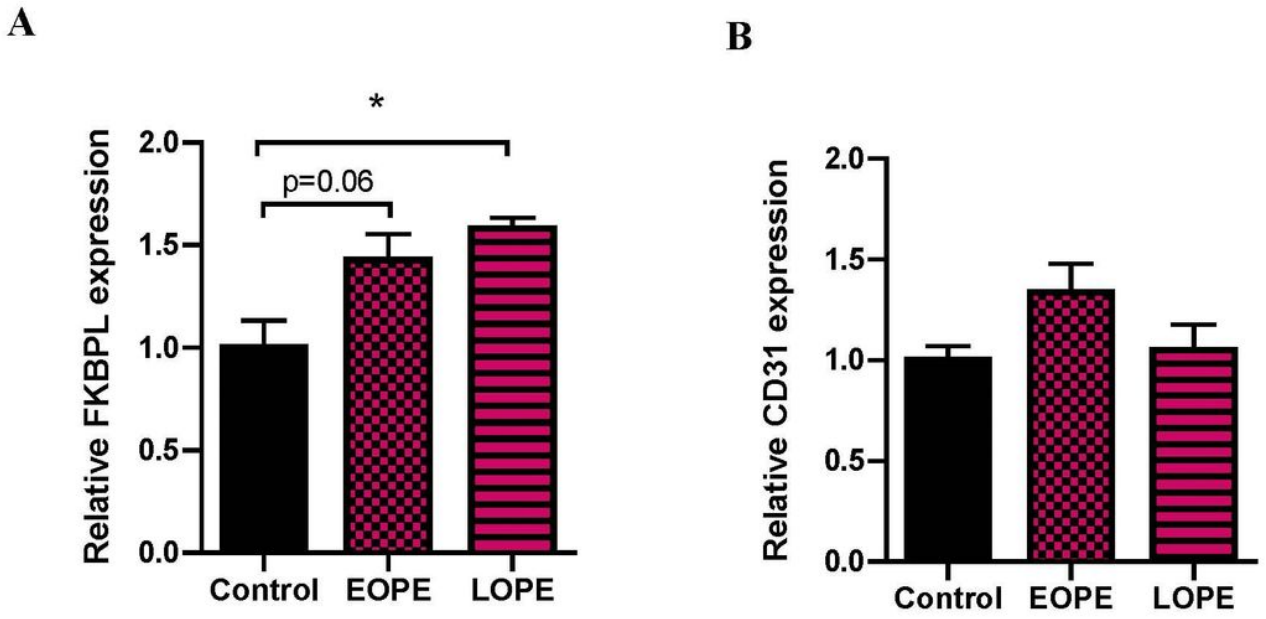

Figure 6

Expression of FKBPL and CD31 in cardiac spheroids treated with plasma from healthy control, early-onset and late-onset preeclampsia patients. Cardiac spheroids generated by co-culturing primary human cardiac fibroblast cells (HCFs) and human coronary artery endothelial cells (HCAECs) were treated with patient plasma from normotensive controls, early-onset preeclampsia and late-onset preeclampsia. Immunofluorescent expression of (A) FKBPL and (B) CD31 in cardiac spheroids was quantified. Data plotted as mean ± SEM, n= 3, Ordinary One-way ANOVA with Tukey's multiple comparison test, *p<0.05.

Supplementary Files

This is a list of supplementary files associated with this preprint. Click to download.

- CRichardsetalAdditionalFile1.pdf